Inorg. Chem. **2007**, *46*, 5276–5282

Inorganic Chemistry
Article

Metal(II) Hexafluorophosphates(V) (M = Sr, Pb) Containing XeF_2-Coordinated Metal Ions $[M(XeF_2)_3](PF_6)_2$, $[Pb_3(XeF_2)_{11}](PF_6)_6$, and $[Sr_3(XeF_2)_{10}](PF_6)_6$

Tina Bunič, Melita Tramšek, Evgeny Goreshnik, Gašper Tavčar, and Boris Žemva*

Department of Inorganic Chemistry and Technology, Jožef Stefan Institute, Jamova 39,
SI−1000 Ljubljana, Slovenia

Received February 7, 2007

From the system $MF_2/PF_5/XeF_2$/anhydrous hydrogen fluoride (aHF), four compounds $[Sr(XeF_2)_3](PF_6)_2$, $[Pb(XeF_2)_3](PF_6)_2$, $[Sr_3(XeF_2)_{10}](PF_6)_6$, and $[Pb_3(XeF_2)_{11}](PF_6)_6$ were isolated and characterized by Raman spectroscopy and X-ray single-crystal diffraction. The $[M(XeF_2)_3](PF_6)_2$ (M = Sr, Pb) compounds are isostructural with the previously reported $[Sr(XeF_2)_3](AsF_6)_2$. The structure of $[Sr_3(XeF_2)_{10}](PF_6)_6$ (space group *C2/c*; $a = 11.778(6)$ Å, $b = 12.497(6)$ Å, $c = 34.60(2)$ Å, $\beta = 95.574(4)°$, $V = 5069(4)$ Å^3, $Z = 4$) contains two crystallographically independent metal centers with a coordination number of 10 and rather unusual coordination spheres in the shape of tetracapped trigonal prisms. The bridging XeF_2 molecules and one bridging PF_6^- anion, which connect the metal centers, form complicated 3D structures. The structure of $[Pb_3(XeF_2)_{11}](PF_6)_6$ (space group *C2/m*; $a = 13.01(3)$ Å, $b = 11.437(4)$ Å, $c = 18.487(7)$ Å, $\beta = 104.374(9)°$, $V = 2665(6)$ Å^3, $Z = 2$) consists of a 3D network of the general formula $\{[Pb_3(XeF_2)_{10}](PF_6)_6\}_n$ and a noncoordinated XeF_2 molecule fixed in the crystal structure only by weak electrostatic interactions. This structure also contains two crystallographically independent Pb atoms. One of them possesses a unique homoleptic environment built up by eight F atoms from eight XeF_2 molecules in the shape of a cube, whereas the second Pb atom with a coordination number of 9 adopts the shape of a tricapped trigonal prism common for lead compounds. $[Pb_3(XeF_2)_{11}](PF_6)_6$ and $[Sr_3(XeF_2)_{10}](PF_6)_6$ are formed when an excess of XeF_2 is used during the process of the crystallization of $[M(XeF_2)_3](PF_6)_2$ from their aHF solutions.

1. Introduction

Metal(II) hexafluorometalates, $M^{n+}(AF_6^-)_n$, where $A = P$, As, Sb, Bi, Ta, Ru, and so forth and n is the oxidation state of the metal, have rather-low lattice energies as a consequence of the anion volume (>100 Å^3).[1] Thus, almost "naked" metal centers surrounded by weakly coordinating AF_6^- anions can therefore interact even with weak ligands, for example XeF_2, forming a whole series of coordination compounds of the type $[M^{n+}(XeF_2)_p](AF_6^-)_n$.[2] The first isolated coordination compound of this type, with PF_6^- as an anion, was $[Ag(XeF_2)_2]PF_6$,[3] which is isostructural with $[(Ag(XeF_2)_2]AsF_6$,[4] the first-known compound with XeF_2 as a ligand to a metal ion.

Recently, the first coordination compounds with PF_6^- as an anion and a metal in a II+ oxidation state were isolated and characterized. $[M(XeF_2)_5](PF_6)_2$ (M = Ca, Cd)[5] were prepared by the reaction of MF_2 and XeF_2 under the pressure of gaseous PF_5 (6.7−8.7 bar) in anhydrous hydrogen fluoride (aHF). Both salts are structurally related. They are not stable in a dynamic vacuum at room temperature and slowly lose XeF_2 and PF_5 yielding MF_2 as the final product.

In this Article, the syntheses, Raman spectra, and crystal structures of four new metal(II) hexafluorophosphates(V) containing XeF_2 as ligands are described.

2. Experimental Section

2.1. General Experimental Procedures. A nickel−Teflon vacuum system was used as previously described.[6] Volatile materials (anhydrous hydrogen fluoride (aHF), PF_5, XeF_2) were manipulated in an all-Teflon vacuum line equipped with

---

* To whom correspondence should be addressed. E-mail: boris.zemva@ijs.si, Phone: + 386 1 477 35 40, Fax: +386 1 477 31 55.

(1) Jenkins, H. D. B.; Roobottom, H. K.; Passmore, J.; Glasser, L. *Inorg. Chem.* **1999**, *38*, 3609−3620.

(2) Tramšek, M.; Žemva, B. *J. Fluorine Chem.* **2006**, *127*, 1275−1284.

(3) Matsumoto, K.; Hagiwara, R.; Ito, Y.; Tamada, O. *Solid State Sci.* **2002**, *4*, 1465−1469.

(4) Hagiwara, R.; Hollander, F.; Maines, C.; Bartlett, N. *J. Solid State Inorg. Chem.* **1991**, *28*, 855−866.

10.1021/ic0702365 CCC: $37.00

Table 1. Crystal Data and Structure Refinement for **I**−**IV**

parameter	$[Sr(XeF_2)_3](PF_6)_2$	$[Pb(XeF_2)_3](PF_6)_2$	$[Sr_3(XeF_2)_{10}](PF_6)_6$	$[Pb_3(XeF_2)_{11}](PF_6)_6$
fw	885.44	1005.01	2825.2	3353.65
T (K)	200	200	200	200
space group	$C2/m$	$C2/m$	$C2/c$	$C2/m$
a (Å)	12.232(6)	12.242(1)	11.778(6)	13.01(3)
b (Å)	11.947(6)	12.0533(8)	12.497(6)	11.437(4)
c (Å)	10.898(5)	10.9607(9)	34.60(2)	18.487(7)
β (deg)	98.801(6)	98.999(4)	95.574(4)	104.374(9)
V (Å^3)	1573(1)	1597.4(2)	5069(4)	2665(6)
Z	4	4	4	2
D_{calcd} (g/cm^3)	3.737	4.179	3.703	4.180
λ (Å)	0.71069	0.71069	0.71069	0.71069
μ (mm^{-1})	10.158	17.195	10.128	16.729
R1, wR2	0.0332, 0.0613	0.0639, 0.1616	0.0726, 0.1958	0.0764, 0.1446
GOF	0.89	1.117	1.074	1.052

Teflon valves. Nonvolatile materials that were sensitive to traces of moisture were handled in the dry argon atmosphere of a glove box with less than 0.1 ppm of water vapor (MBraun: Garching, Germany). A Teflon−FEP (fluorinated ethylene propylene) reaction vessel equipped with a Teflon valve and a Teflon-covered mixing bar was used for the syntheses. A T-shaped FEP reaction vessel, constructed from one large FEP tube (i.d. = 16 mm) and one smaller FEP tube (i.d. = 4 mm) joined at a right angle and equipped with a Teflon valve, was used for recrystallizations.

2.2. Reagents. SrF_2 (Alfa Aesar, 99.99%), PbF_2 (Merck, Suprapur), and fluorine (Solvay, 99.98%) were used as purchased. PF_5 was prepared by fluorination of P_2O_5 powder under high pressure, as previously described.[7] Its purity was checked by IR spectroscopy. XeF_2 was prepared by the photochemical reaction between xenon and fluorine at room temperature.[8] aHF (Fluka, purum) was treated with K_2NiF_6 (Ozark-Mahoning, 99%) for several days prior to use. Caution: aHF and PF_5 must be handled in a well-ventilated hood and protective clothing must be worn all the times! The experimentalist must become familiar with these reagents and the hazards associated with them. Fresh tubes of calcium gluconate gel should always be on hand for the fast treatment of skin exposed to these reagents. For treatment of HF injuries see the references.[9]

2.3. Syntheses and Preparation of Single Crystals. 2.3.1. Synthesis of $[M(XeF_2)_3](PF_6)_2$. MF_2 and XeF_2 were weighed into the reaction vessel inside the dry box. The reaction vessel was cooled with liquid nitrogen, and aHF was added at −196 °C. Then the reaction vessel was warmed up to room temperature and weighed. The vessel was cooled again to −196 °C, and an excess of PF_5 was added. The vessel was kept at room temperature for at least 24 h, and the reaction mixture was stirred continuously. aHF and unreacted XeF_2 and PF_5 were pumped off at room temperature. Details of the syntheses were as follows: SrF_2 (0.124 g, 0.99 mmol); XeF_2 (0.838 g, 4.95 mmol); PF_5 (1.255 g, 9.96 mmol); product $[Sr(XeF_2)_3](PF_6)_2$ (0.877 g, 0.99 mmol); PbF_2 (0.246 g, 1.00 mmol); XeF_2 (0.893 g, 5.27 mmol); PF_5 (0.599 g, 4.75 mmol); product $[Pb(XeF_2)_3](PF_6)_2$ (1.012 g, 1.01 mmol).

2.3.2. Preparation of Single Crystals. 2.3.2.1. $[M(XeF_2)_3](PF_6)_2$. Approximately 100 mg of $[M(XeF_2)_3](PF_6)_2$ (section 2.3.1) was transferred in the dry box into the T-shaped crystallization vessel (section 2.1). aHF was added on the vacuum line, and a saturated solution was prepared. This solution was decanted into the narrower part of the reaction vessel, which was left at room temperature while the wider part was slightly cooled to generate a small temperature gradient. The crystallization proceeded for several days. Crystals were isolated by pumping off the aHF. Inside the drybox, they were put in perfluorinated oil (ABCR, FO5960), selected under a microscope, and transferred into a cold nitrogen stream on the X-ray diffractometer.

2.3.2.2. $[Sr_3(XeF_2)_{10}](PF_6)_6$ and $[Pb_3(XeF_2)_{11}](PF_6)_6$. Approximately 100 mg of the starting compounds $[M(XeF_2)_3](PF_6)_2$ (M = Sr or Pb) and approximately 100 mg of XeF_2 were transferred into the crystallization vessel in the dry box. In this way, the mole ratio between M and total XeF_2 was in the range from 1:27 (Sr) to 1:31 (Pb). Crystals of $[Sr_3(XeF_2)_{10}](PF_6)_6$ were prepared also by a direct reaction between SrF_2 (0.036 g, 0.29 mmol), XeF_2 (0.315 g, 1.86 mmol), and PF_5 (∼2.5 mmol) in aHF in the wider part of the crystallization vessel. The clear solution was decanted into the narrower part. Crystallization and crystal handling were the same as described above.

2.4. Raman Spectroscopy. Raman spectra of powdered samples in sealed quartz capillaries were taken on a Renishaw Raman Imaging Microscope System 1000 with the 632.8 nm exciting line of a He−Ne laser. The geometry for all of the Raman experiments was 180° backscattering with a laser power of 25 mW.

2.5. Determination of Crystal Structures. Data were collected on Rigaku AFC7 diffractometer equipped with a Mercury CCD area detector using graphite monochromated Mo Kα radiation at −73 °C. The data were corrected for Lorentz and polarization effects. A multiscan absorption correction was applied to all of the data sets. All of the structures were solved by direct methods using the *SIR92*[10] program implemented in the program package *TeXsan*[11] and refined with the *SHELXL-97*[12] software (program packages

---

(5) Bunič, T.; Tavčar, G.; Tramšek, M.; Žemva, B. *Inorg. Chem.* **2006**, *45*, 1038−1042.

(6) Mazej, Z.; Benkič, P.; Lutar, K.; Žemva, B. *J. Fluorine Chem.* **2001**, *112*, 173−183.

(7) Jesih, A.; Žemva, B. *Vestn. Slov. Kem. Druš.* **1986**, *33*, 25−28.

(8) Šmalc, A.; Lutar, K. *Inorganic Syntheses*; Grimes R. N., Ed.; John Wiley & Sons: New York, 1992, Vol. 29, pp 1−4.

(9) Peters, D.; Miethchen, R. *J. Fluorine Chem.* **1996**, *79*, 161−165.

Table 2. Selected Bond Distances (Angstroms) in $[Sr(XeF_2)_3](PF_6)_2$

Sr1−F3b, Sr1−F3b[a]	2.466(4)	Sr1−F11, Sr1−F11[a]	2.673(4)
Sr1−F3a[b], Sr1−F3a[c]	2.508(4)	Sr1−F1	2.556(6)
Sr1−F2	2.516(5)	Sr1−F24	2.541(6)
Xe1−F1, Xe1−F1[d]	1.996(6)	Xe2−F2, Xe2−F2[e]	1.988(5)
Xe3−F3b	1.971(4)	Xe3−F3a	2.007(4)
P2−F23, P2−F23[a]	1.591(4)	P1−F13, P1−F13[f]	1.582(5)
P1−F11, P1−F11[f]	1.641(4)	P1−F12, P1−F12[f]	1.576(5)
P2−F21	1.561(7)	P2−F22	1.599(6)
P2−F25	1.589(5)	P2−F24	1.663(6)

Symmetry codes: [a] $x, 1 - y, z$. [b] $x - {}^{1}/_{2}, y - {}^{1}/_{2}, z$. [c] $x - {}^{1}/_{2}, {}^{3}/_{2} - y, z$. [d] $-x, 1 - y, 1 - z$. [e] $1 - x, 1 - y, 1 - z$. [f] ${}^{1}/_{2} - x, {}^{1}/_{2} - y, 1 - z$.

Table 3. Selected Bond Distances (Angstroms) in $[Pb(XeF_2)_3](PF_6)_2$

Pb1−F3b, Pb1−F3b[a]	2.468(8)	Pb1−F2	2.53(2)
Pb1−F3a, Pb1−F3a[a]	2.549(8)	Pb1−F24	2.56(1)
Pb1−F11, Pb1−F11[a]	2.79(1)	Pb1−F1	2.62(1)
Xe1−F1, Xe1−F1[b]	1.99(1)	Xe2−F2, Xe2−F2[c]	1.99(1)
Xe3−F3a[d]	2.003(8)	Xe3−F3b	1.981(9)
P1−F12, P1−F12[e]	1.56(1)	P1−F11, P1−F11[e]	1.629(9)
P2−F23, P2−F23[a]	1.571(9)	P1−F13, P1−F13[e]	1.56(1)
P2−F21	1.57(2)	P2−F25	1.59(1)
P2−F22	1.60(1)	P2−F24	1.67(1)

Symmetry codes: [a] $x, -y, z$. [b] $1 - x, -y, -z$. [c] $-x, -y, -z$. [d] $x - {}^{1}/_{2}, {}^{1}/_{2} + y, z$. [e] ${}^{1}/_{2} - x, {}^{1}/_{2} - y, -z$.

Table 4. Selected Bond Distances (Angstroms) in $[Sr_3(XeF_2)_{10}](PF_6)_6$

Sr1−F3a	2.50(1)	Sr1−F1a	2.55(1)	Sr1−F1b[a]	2.53(1)
Sr1−F5b	2.52(1)	Sr1−F15	2.57(1)	Sr1−F36	2.53(1)
Sr1−F3b[b]	2.54(1)	Sr1−F25	2.79(1)	Sr1−F22	2.63(1)
Sr2−F4b[b]	2.53(1)			Sr1−F2a	2.64(1)
Sr2−F4b[c]					
Sr2−F4a	2.57(1)	Sr2−F5a[e]	2.53(1)		
Sr2−F4a[d]		Sr2−F5a[f]			
Sr2−F16[b]	2.63(1)	Sr2−F2b	2.62(1)		
Sr2−F16[c]		Sr2−F2b[d]			
Xe1−F1a	1.93(1)	Xe3−F3a	1.97(1)	Xe4−F4a	1.98(1)
Xe1−F1b	2.01(1)	Xe3−F3b	2.01(1)	Xe4−F4b	2.03(1)
Xe2−F2a	2.00(1)			Xe5−F5b	1.98(1)
Xe2−F2b	2.00(1)			Xe5−F5a	2.00(1)
P1−F11	1.56(2)	P2−F21	1.58(1)	P3−F31	1.53(2)
P1−F12	1.55(1)	P2−F23	1.59(1)	P3−F32	1.57(2)
P1−F13	1.56(2)	P2−F24	1.59(1)	P3−F33	1.57(2)
P1−F14	1.56(2)	P2−F25	1.62(1)	P3−F34	1.57(2)
P1−F16	1.62(1)	P2−F22	1.62(1)	P3−F35	1.60(1)
P1−F15	1.63(1)	P2−F26	1.63(1)	P3−F36	1.64(1)

Symmetry codes: [a] ${}^{1}/_{2} + x, y - {}^{1}/_{2}, z$. [b] ${}^{1}/_{2} + x, {}^{1}/_{2} + y, z$. [c] ${}^{3}/_{2} - x, {}^{1}/_{2} + y, {}^{3}/_{2} - z$. [d] $2 - x, y, {}^{3}/_{2} - z$. [e] $1 + x, y, z$. [f] $1 - x, y, {}^{3}/_{2} - z$.

TeXsan and *WinGX*).[13] The figures were prepared using *DIAMOND* version 3.1 software.[14] The crystal data and the details of the structure refinements for **I**−**IV** are given in Table 1, and selected distances for **I**, **II**, **III**, and **IV** are placed in Tables 2−5, respectively.

3. Results and Discussion

3.1. Syntheses. The claim in the literature[15] that $XeF_2 \cdot PF_5$ can be isolated at −78 °C and $2XeF_2 \cdot PF_5$ at room temperature was not confirmed in our laboratory. PF_5 is not a strong enough Lewis acid either to withdraw F^- from the moderately strong Lewis base XeF_2 to form a XeF^+ or a $Xe_2F_3^+$ salt or to at least form an adduct with it. Therefore, the coordination compounds of the type $[M(XeF_2)_3](PF_6)_2$ (M = Sr, Pb) can be prepared directly by the reaction between the corresponding binary fluoride, XeF_2 and gaseous PF_5 in aHF as a solvent. Because the solubility of PF_5 in aHF is poor,[16] a high pressure of PF_5 (5.3−7.3 bar) must be employed. $[M(XeF_2)_3](PF_6)_2$ (M = Sr, Pb) are white solids that slowly lose XeF_2 and PF_5 under a dynamic vacuum at room temperature. To obtain the compounds with appropriate stoichiometry, it is necessary to remove aHF and the excess of PF_5 carefully at a lower temperature (∼ −30 °C) and the excess of XeF_2 at room temperature. The change in weight of the product as a function of time of pumping must be carefully monitored. A stable product is obtained when the curve of the weight loss versus time of pumping approaches zero.

The coordination compounds with the higher amounts of XeF_2, such as $[Sr_3(XeF_2)_{10}](PF_6)_6$ and $[Pb_3(XeF_2)_{11}](PF_6)_6$, were prepared using a higher molar ratio of XeF_2 to M^{2+}. The best results were obtained by adding extra XeF_2 to $[M(XeF_2)_3](PF_6)_2$ and by dissolving these solid mixtures in aHF. The crystals of $[Sr_3(XeF_2)_{10}](PF_6)_6$ and $[Pb_3(XeF_2)_{11}](PF_6)_6$ were prepared by the crystallizations from these solutions, in a manner similar to that described in section 2.3.2.

3.2. Crystal Structures. 3.2.1. Crystal Structures of $[Sr(XeF_2)_3](PF_6)_2$ and $[Pb(XeF_2)_3](PF_6)_2$. The cations of strontium and lead (M^{2+}) have rather similar cationic radii ($r_{Sr^{2+}} = 1.45$ Å, $r_{Pb^{2+}} = 1.49$ Å; CN = 9 in both cases).[17] Therefore, it is not surprising that some of their coordination compounds are isostructural. This is the case for the compounds with the general formula $[M(XeF_2)_3](AF_6)_2$, where M = Sr, Pb and A = As.[18] The discussed compounds are also isostructural with the above-mentioned ones. Six F atoms from six bridging XeF_2 molecules and three F atoms from one terminal and two bridging PF_6 units form a tricapped trigonal prism around the metal atom (Figure 1). As a result of six bridging XeF_2 and two bridging PF_6^- units, double layers are formed (Figure 2). Weak electrostatic Xe$\cdots$F(PF_6) interactions link such layers in a 3D network.

In both structures, XeF_2 molecules (Xe1 and Xe2) are linear and symmetric, while XeF_2 (Xe3) molecules are slightly distorted from linear symmetry with the F3a−Xe3−F3b angles being 178.6(2)° (Sr) and 177.8(4)° (Pb). The main reason for this distortion is the relatively strong electrostatic interaction between the positive Xe3 center and the negative F23 atom from the terminal PF_6^- anion in the next slab at a distance of 3.221(7) Å. In crystalline XeF_2, each Xe atom

---

(10) Altomare, A.; Cascarano, G.; Giacovazzo, C.; Guagliardi, A. *SIR92*, *J. Appl. Cryst.* **1993**, *26*, 343−350.

(11) *TeXsan for Windows*, version 1.06; Single Crystal Structure Analysis Software MSC, 9009; Molecular Structure Corporation: New Trails Drive, The Woodlands, TX 77381, U.S.A., 1997−1999.

(12) Scheldrick, G. M.; *SHELXL-97*; University of Göttingen: Göttingen, Germany, 1997.

(13) Farrugia, L. J. *J. Appl. Cryst.* **1999**, *32*, 837−838.

(14) *DIAMOND*, version 3.1.; Crystal Impact GbR: Bonn, Germany, 2004−2005.

(15) Meinert, H.; Rüdiger, S. *Z. Chem.* **1969**, *9*, 71−71.

(16) Grütner, B.; Dove, M. F. A.; Clifford, A. F. *Chemistry in Anhydrous, Prototropic Inorganic Solvents, Vol. II, Inorganic Chemistry in Liquid Hydrogen Cyanide and Liquid Hydrogen Fluoride*; Pergamon Press: Oxford, U.K., 1971; p 252.

(17) Shanon, R. D. *Acta Crystallogr. Sect., A* **1976**, *32*, 751−767.

(18) Tramšek, M.; Benkič P.; Žemva, B. *Solid State Sci.* **2002**, *4*, 9−14.

Table 5. Selected Bond Distances (Angstroms) in $[Pb_3(XeF_2)_{11}](PF_6)_6$

Pb1−F2[a] Pb1−F2[b] Pb1−F2 Pb1−F2[c]			2.49(1)		
Pb1−F4a Pb1−F4a[a] Pb1−F4a[c] Pb1−F4a[b]			2.54(1)		
Pb2−F3a Pb2−F3a[d]	2.53(1)	Pb2−F31	2.53(2)		
Pb2−F3b[e] Pb2−F3b[f]	2.50(1)	Pb2−F21	2.69(2)		
Pb2−F4b Pb2−F4b[d]	2.63(1)	Pb2−F11	2.75(2)		
Xe1−F1 Xe1−F1[g]	1.93(3)	Xe2−F2 Xe2−F2[h]	1.99(1)		
Xe3−F3a	2.02(1)	Xe4−F4a	2.00(1)		
Xe3−F3b	2.00(1)	Xe4−F4b	1.98(1)		
P1−F12 P1−F12[d]	1.57(2)	P2−F22 P2−F22[d]	1.53(2)		
P2−F23 P2−F23[d]	1.52(2)	P3−F34 P3−F34[d]	1.58(1)		
P1−F14	1.60(2)	P2−F24	1.62(2)	P3−F32	1.56(2)
P1−F11	1.61(2)	P2−F21	1.64(2)	P3−F33	1.56(2)
P1−F15	1.61(2)			P3−F35	1.57(2)
P1−F13	1.62(2)			P3−F31	1.64(2)

Symmetry codes: [a] x, $1 - y$, z. [b] $2 - x$, y, $1 - z$. [c] $2 - x$, $1 - y$, $1 - z$. [d] x, $-y$, z. [e] $x - 1/2$, $y - 1/2$, z. [f] $x - 1/2$, $1/2 - y$, z. [g] $2 - x$, $-y$, $1 - z$. [h] $5/2 - x$, $1/2 - y$, $1 - z$.

has eight F atoms from the neighboring XeF_2 molecules at a distance of 3.42 Å.[19] The interaction between Xe3 and F23 can be also seen from the angles F23−P2−F23, which are 177.4(4)°(Sr) and 176.6(9)° (Pb).

3.2.2. Crystal Structure of $[Sr_3(XeF_2)_{10}](PF_6)_6$. This structure contains two crystallographically independent metal centers. Both possess rather unusual coordination spheres in the shape of tetracapped trigonal prisms with an average Sr−F distance of 2.58(1) Å. Two rectangular planes in each metal coordination polyhedron are monocapped, while the third one is bicapped (Figure 3). The coordination environment of the Sr1 atom consists of six F atoms from bridging XeF_2 molecules, one F atom from the terminal anion, and one more F atom from the bridging PF_6^- unit, while the last two F atoms originate from the third PF_6^- unit coordinated to the Sr atom in a chelate manner (Figure 3, left). The area surrounding the Sr2 atom includes eight F atoms from bridging XeF_2 and two more F atoms from two PF_6^- bridging anions (Figure 3, right). Because of the location of the Sr2 atom on a 4e special position (all of the other atoms are located on general 8f Wyckoff positions), the ratio between the amount of Sr1/Sr2 atoms appears to be 2:1. The formula for the Sr1 surrounding is $Sr(1)(XeF_2)_3(PF_6)_{2.5}$, whereas the formula for the Sr2 environment can be written as $Sr(2)(XeF_2)_4(PF_6)$, which gives the overall formula $[Sr_3(XeF_2)_{10}](PF_6)_6$. Five crystallographically independent bridging XeF_2 molecules and one bridging PF_6^- anion form a complicated 3D network.

Some XeF_2 moieties demonstrate noticeable asymmetry in their geometry (Table 4). There are two possible reasons, which could cause such behavior: a different bridging role (connecting Sr1⋯Sr1, Sr2⋯Sr2, or Sr1⋯Sr2 metal centers), and participation of F atoms of one XeF_2 molecule in the formation of weak electrostatic F⋯Xe interactions with Xe atoms of the other XeF_2 molecules with distances of 3.3−3.4 Å.

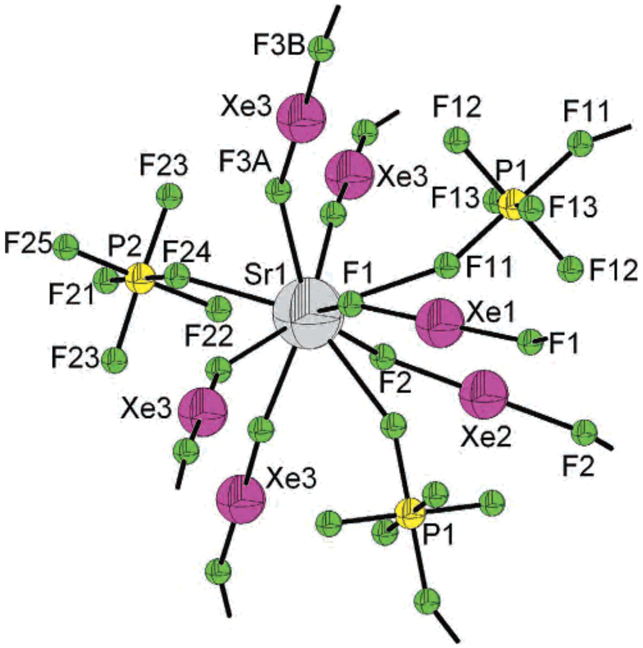

Figure 1. Basic unit in the structure of $[Sr(XeF_2)_3](PF_6)_2$ showing the coordination sphere around the Sr atom.

In the case of Sr1, the terminal $P(3)F_6^-$ anion successfully competes with the XeF_2 molecules as a ligand to the metal center. The shortest Sr−F(Xe) distance is 2.50(1) Å, while the shortest Sr1−F(P3) distance is 2.53(1) Å. Furthermore, the bridging anion $P(1)F_6^-$ has shorter Sr1−F distance (2.53(1) Å) as is the longest Sr1−F(Xe2) distance (2.64(1) Å). It is clear that the negative charges on the F atoms of the XeF_2 ligands or AF_6^- anions are not the only parameters that determine the M−F(Xe, A) distance. The properties of the cation (fluoride affinity, effective nuclear charge, effective volume, Lewis acidity, covalency of M−F bond, coordination number, etc.) as well as the properties of the anion (Lewis basicity, size of the anion, etc.) should also be considered. In the case of the Sr2 polyhedron, the Sr2−F(Xe) distances are the shortest, while the Sr2−F(P1) ones are the longest. It appears that the strongly electronegative F atoms of the XeF_2 molecules easily compete with the less-electronegative F atoms from the bridging $P(1)F_6^-$ anion.

Four of the five crystallografically different XeF_2 molecules are slightly distorted from linearity with the F−Xe−F angles ranging from 177.2(5)° to 178.6(5)° (the F−Xe4−F angle is 179.4(5)) and the two nonequivalent Xe−F distances varying from 1.93(1) to 2.01(1) Å. The main reasons for these distortions are the interactions of the positive Xe centers with the negative F atoms of the anions (Xe⋯F = 3.17−3.30 Å).

3.2.3. Crystal Structure of $[Pb_3(XeF_2)_{11}](PF_6)_6$. The structure of $[Pb_3(XeF_2)_{11}](PF_6)_6$ contains two crystallographically independent Pb atoms (Figure 4). Eight F atoms, belonging to eight bridging XeF_2 molecules, form a unique

---

(19) Agron, P. A.; Begun, G. M.; Levy, H. A.; Mason, A. A.; Jones, C. G.; Smith, D. F. *Science* **1963**, *139*, 842−844.

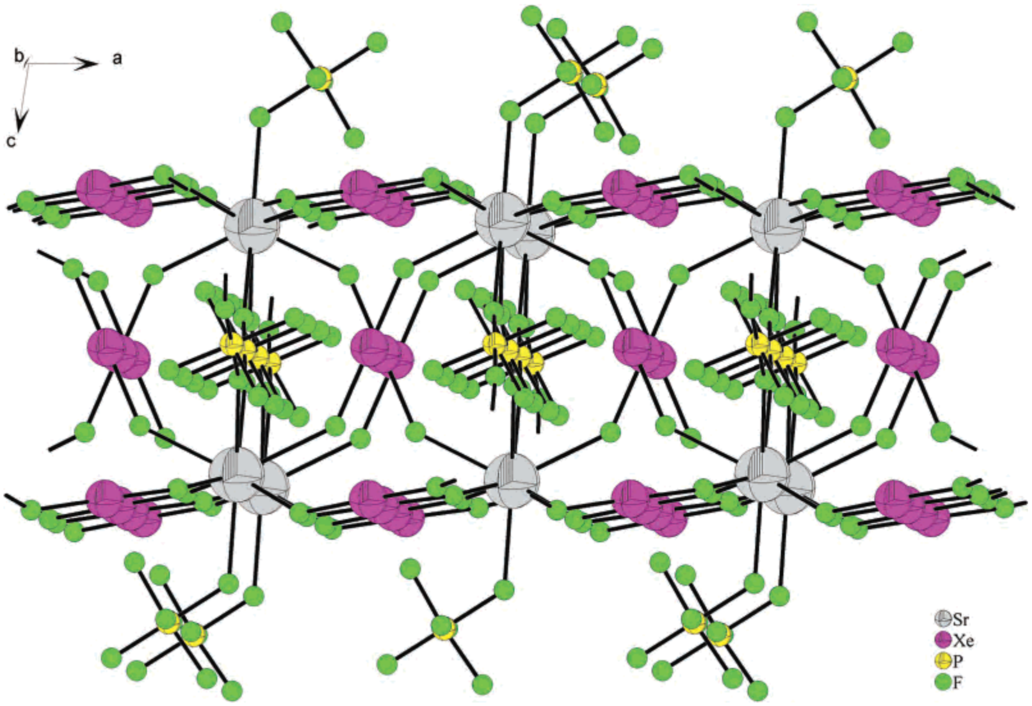

Figure 2. Double layer in the structure of $[Sr(XeF_2)_3](PF_6)_2$.

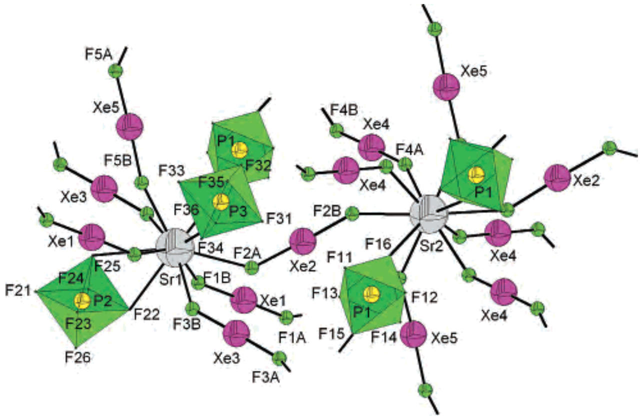

Figure 3. Coordination spheres of the Sr atoms (Sr1 and Sr2) in the structure of $[Sr_3(XeF_2)_{10}](PF_6)_6$.

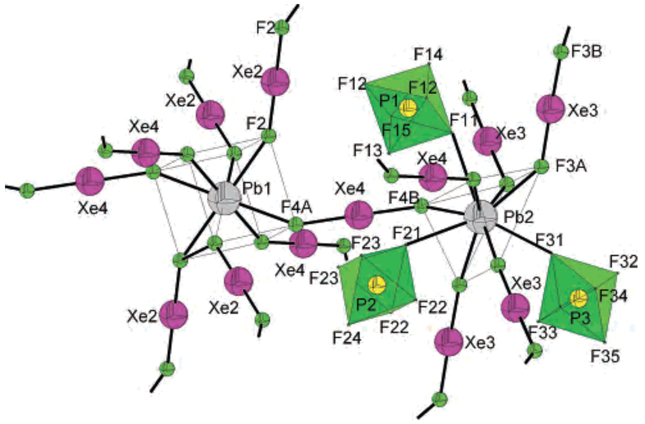

Figure 4. Coordination spheres around Pb atoms (Pb1 and Pb2) in the structure of $[Pb_3(XeF_2)_{11}](PF_6)_6$.

homoleptic cubic environment for the Pb1 atom. The Pb1−F distances form two sets with $r = 4 \times 2.49(1)$ and $4 \times 2.54(1)$ Å (Table 5). The coordination sphere of the Pb2 atom adopts a shape common for lead compounds, that is, a tricapped trigonal prism composed of six F atoms from six bridging XeF_2 molecules and three F atoms from three terminal PF_6 units. Bond lengths of Pb2−F(Xe) appear to be 2.50(1)−2.54(1) Å, and those of Pb2−F(P) appear to be 2.50(1)−2.75(2) Å.

The bridging XeF_2 molecules are responsible for the formation of a 3D network. The general formula for the area surrounding Pb1 is $Pb(XeF_2)_4$, while the environment of Pb2 can be written with the general formula $Pb(XeF_2)_3(PF_6)_3$. Taking into account that the ratio of Pb1/Pb2 in each unit cell is 1:2 because of the location of Pb1 and Pb2 atoms on 2d and 4i Wyckoff positions, respectively. The general formula of the 3D network is $[Pb_3(XeF_2)_{10}](PF_6)_6$. The view of the *ac* plane shows infinite chains of $[(Pb(1)(XeF_2)_4]_n$ (Figure 5). Each chain is connected to two double ribbons that contain the Pb2 atoms.

The last XeF_2 molecule (Xe1) does not participate in the metal coordination. It is fixed in the crystal space only by a weak Xe···F interaction (Figure 6). The lengths of these contacts are in the range of 3.35−3.37 Å. Similar “free” XeF_2 molecules were found earlier, for example in the structure of $Ba(XeF_2)_5(SbF_6)_2$.[20]

The Xe−F distances in the structure of $[Pb_3(XeF_2)_{11}](PF_6)_6$ roughly correlate with the XeF_2 coordination role. The Xe(2)F_2 and Xe(3)F_2 moieties, which are bonded to the pair of Pb1−Pb1 and Pb2−Pb2 atoms, respectively, exhibit symmetrical geometries, whereas the Xe(4)F_2 bridge between the Pb1 and Pb2 atoms appears to be rather asymmetrical.

---

(20) Turičnik, A.; Benkič, P.; Žemva, B. *Inorg. Chem.* **2002**, *41*, 5521−5524.

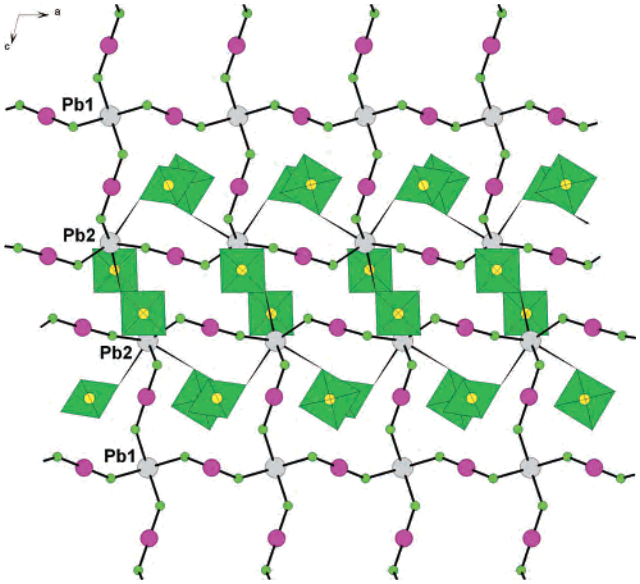

Figure 5. Projection of the structure of $[Pb_3(XeF_2)_{11}](PF_6)_6$ on the *ac* plane.

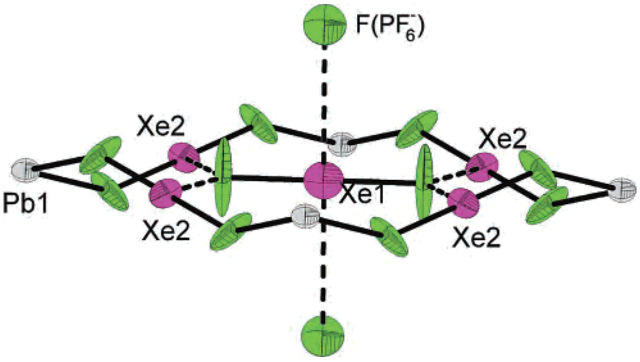

Figure 6. "Free" XeF_2 molecule in the structure of $[Pb_3(XeF_2)_{11}](PF_6)_6$.

The "free" $Xe(1)F_2$ molecule contains Xe−F distances that are apparently shorter than those in the crystalline XeF_2 (Table 5).

In the coordination spheres of the Pb1 and Pb2 polyhedra, the Pb−F distances are as expected for ionic Pb−F bonds (CN = 9). The Pb−F distances in PbF_2 are in the range from 2.45 to 3.03 Å.[21] The coordination polyhedra of Pb1 and Pb2 do not show sterical activity of the lone pair at the Pb(II) atom, as observed in the PbO structure.[22] The coordination number of Pb1 is only 8. This is most probably a consequence of the stronger interaction of eight XeF_2 molecules with the central atom, while in the case of Pb2, again the usual coordination number of 9 is adopted. The reason for the lower coordination number of lead, when compared to strontium, is the higher absolute electronegativity of Sr^{2+} (27.3 eV) relative to Pb^{2+} (23.49 eV).[23]

The XeF_2 molecules of Xe2 are linear and symmetric, while the XeF_2 molecules of Xe3 and Xe4 are slightly distorted and are neither linear nor symmetric. The XeF_2 of Xe1 is placed in an empty space in the 16-membered ring formed by four $Xe(2)F_2$ molecules and four Pb1 atoms. The $Xe(1)F_2$ molecule is kept in place by four weak interactions between the positive Xe2 atoms and the negative F atoms from $Xe(1)F_2$ at a distance of 3.38(1) Å and two interactions with F atoms from the $P(1)F_6^-$ anion at a distance of 3.35(2) Å.

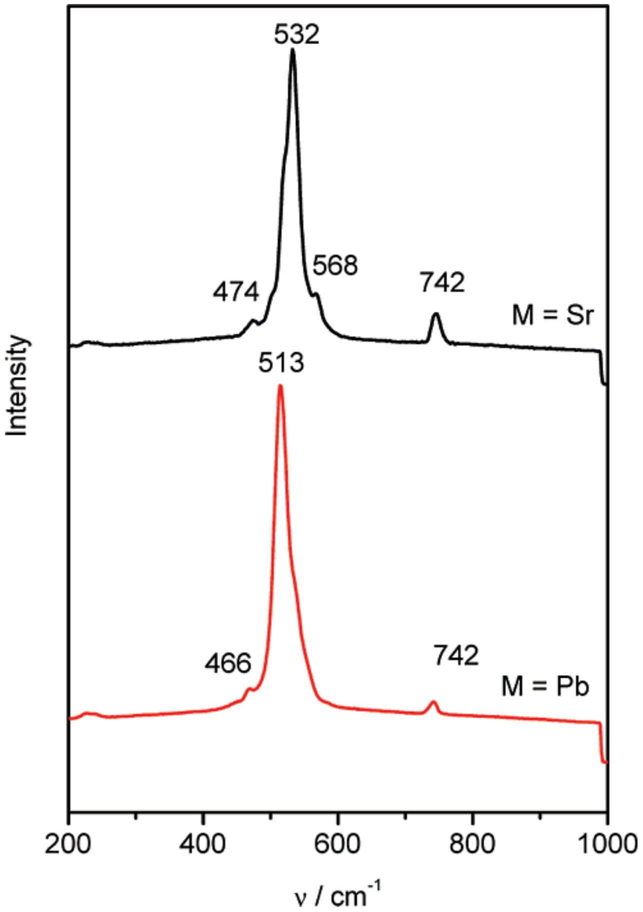

Figure 7. Raman spectra of $[M(XeF_2)_3](PF_6)_2$.

The Xe1−F distance is rather short. The main reason for this is that the thermal motion of the F1 atoms is large, perpendicular to the plane of the 16-membered ring. In the plane of the ring, the motion of the F1 atoms is restricted because of their interactions with four Xe2 atoms. Of course, taking into account the high standard deviations, the Xe−F bond lengths are not significantly different from the crystalline XeF_2.

3.3. Raman Spectroscopy. 3.3.1. Raman spectra of $[M(XeF_2)_3](PF_6)_2$. The Raman spectra (Figure 7) for $[M(XeF_2)_3](PF_6)_2$ (M = Sr, Pb) are in accord with their structures. The high polarizability of xenon usually results in intense Raman bands for the symmetric Xe−F stretching modes. Raman P−F vibrations are usually far less intense because of the lower polarizabilities of these small atoms. The symmetric (ν_1) stretching mode for solid XeF_2 is close to 497 cm^{-1}.[19] In accordance with the findings for the XeF_2 complexes with XeF_5^+ salts,[24,25] it is expected that the ν_1(Xe−F) of bridging XeF_2 would be close to the symmetric (ν_1) stretching mode for solid XeF_2. However, each of the

---

(21) Boldrini, P.; Loopstra, B. O. *Acta Cryst.* **1967**, *22*, 744−745.
(22) Leciejewicz, J. *Acta Cryst.* **1961**, *14*, 66.
(23) Pearson, R. G. *Inorg. Chem.* **1988**, *27*, 734−740.
(24) Žemva, B.; Jesih, A.; Templeton, D. H.; Zalkin, A.; Cheetham, A. K.; Bartlett, N. *J. Am. Chem. Soc.*, **1987**, *109*, 7420−7427.
(25) Žemva, B.; Golič, L.; Slivnik, J. *Vestn. Slov. Kem. Druš.* **1983**, *30*, 365−376.

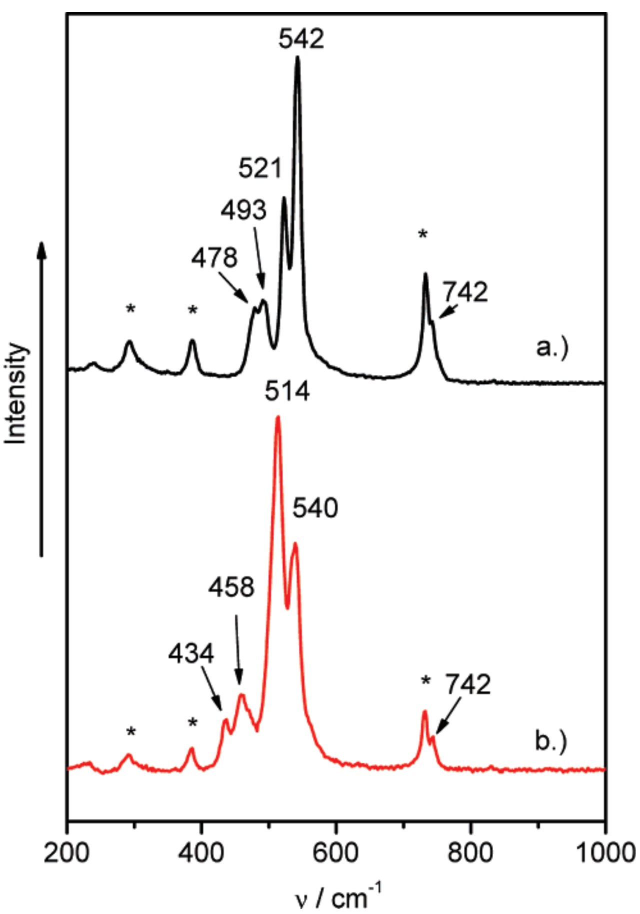

Figure 8. Raman spectra of $[Sr_3(XeF_2)_{10}](PF_6)_6$ (a) and $[Pb_3(XeF_2)_{11}](PF_6)_6$ (b) (asterisk denotes a peak originating from a fluorinated ethylene propylene (FEP) reaction vessel).

bridging XeF_2 molecules in the $[M(XeF_2)_3](PF_6)_2$ compounds is anchored between two metal centers, which causes the increase of the value of ν_1(Xe−F) to 513 cm^{-1} for Pb and to 532 cm^{-1} for Sr. These values are in perfect agreement with the isostructural compounds $[M(XeF_2)_3](AsF_6)_2$ (M = Sr, Pb), where ν_1(Xe−F) is 514 cm^{-1} for the Pb compound and 531 cm^{-1} for the Sr compound.[18] The 17 cm^{-1} higher value of the ν_1 mode of XeF_2 in the case of Sr could be attributed to the higher absolute electronegativity of the Sr^{2+} cation compared to that of the Pb^{2+} cation, as was already mentioned in the discussion of the crystal structures (section 3.2.3).

Because ν_1 of O_h PF_6^- occurs at 756 cm^{-1},[26] the band at 742 cm^{-1} (Pb and Sr) can be confidently assigned to the symmetric stretching mode of the anion. The symmetry of PF_6^- is no longer O_h, and more bands are expected. The symmetric stretching vibration of PF_6^- (ν_1) is very weak in comparison to the Xe−F stretching vibrations; therefore, the other bands were not observed.

3.3.2. Raman spectra of $[Sr_3(XeF_2)_{10}](PF_6)_6$ and $[Pb_3(XeF_2)_{11}](PF_6)_6$. The Raman spectra of $[Sr_3(XeF_2)_{10}](PF_6)_6$ and $[Pb_3(XeF_2)_{11}](PF_6)_6$ are shown in Figure 8. The most prominent features of these spectra are the intense symmetric stretching modes of the more- or less-distorted XeF_2 molecules, which bridge the metal centers.

In the case of $[Sr_3(XeF_2)_{10}](PF_6)_6$, the strongest Raman band at 542 cm^{-1} might be assigned to the symmetric stretching vibration of the shorter Xe−F bond in the most-distorted bridging $Xe(1)F_2$ molecule with an Xe−F distance of 1.93(1) Å. The band at 478 cm^{-1} might be assigned to the symmetric stretching vibration of the longer Xe(1)−F bond of 2.01(1) Å. The bands at 521 and at 493 cm^{-1} might be assigned to the symmetric stretching mode of the other less-distorted XeF_2 molecules with the shorter and the longer Xe−F bonds, respectively. The Raman bands at 542 and at 478 cm^{-1} demonstrate that the bridging $Xe(1)F_2$ molecule is the most-distorted XeF_2 molecule found, up to now. The highest symmetric stretching frequency assigned to the bridging XeF_2 molecule was until now at 531 cm^{-1}.[18] When $[Sr_3(XeF_2)_{10}](PF_6)_6$ is decomposed under a dynamic vacuum at room temperature, all of the peaks become smaller and finally disappear. A new peak at 532 cm^{-1} appears. This peak is a characteristic of $[Sr(XeF_2)_3](PF_6)_2$.

In the case of $[Pb_3(XeF_2)_{11}](PF_6)_6$, there are two sets of bands at 540 and 434 cm^{-1} and at 514 and 458 cm^{-1} representing the symmetric stretching vibrations of the $Xe(4)F_2$ molecule, which is the most distorted, and the symmetric stretching vibrations of all of the other only slightly distorted bridging XeF_2 molecules, respectively. The band of “free” XeF_2 is probably smaller and therefore hidden under strong peak at 514 cm^{-1}. During the decomposition of $[Pb_3(XeF_2)_{11}](PF_6)_6$ in a dynamic vacuum at room temperature, the 1:3 compound is formed. It shows only symmetric stretching vibrations of bridging XeF_2 molecules at 513 cm^{-1}.

The band at 742 cm^{-1} (Sr and Pb) can be confidently assigned to the symmetric stretching mode of the anion (section 3.3.1.).

To prove that the Raman spectrum of the bulk really belongs to the same compound that was structurally characterized, both characterizations were done on the same crystal.

Dedication. The authors dedicate this Article to Prof. Neil Bartlett on the occasion of his 75th birthday. Prof. Neil Bartlett has inspired the group of fluorine chemists at Jožef Stefan Institute in Ljubljana, Slovenia, for the last 35 years with his excellent achievements in the field of fluorine chemistry, especially in noble metals and noble gas chemistry. The authors are grateful to Prof. Bartlett for his scientific guidance and warm friendship.

Acknowledgment. The authors gratefully acknowledge the Slovenian Research Agency (ARRS) for the financial support of the Research Program P1-0045 (Inorganic Chemistry and Technology).

Supporting Information Available: X-ray crystallographic files in CIF format. This material is available free of charge via the Internet at http://pubs.acs.org.

IC0702365

---

(26) Heyns, A. M. *Spectrochim. Acta* **1977**, *33A*, 315−322.